



ELSEVIER

Available online at www.sciencedirect.com

SCIENCE @ DIRECT®

Physica A 332 (2004) 123–140

PHYSICA A

www.elsevier.com/locate/physa

Frequency dependent stochastic resonance in a model for intracellular Ca^{2+} oscillations can be explained by local divergence

Matjaž Perc, Marko Marhl*

Department of Physics, Faculty of Education, University of Maribor, Koroška cesta 160, SI-2000 Maribor, Slovenia

Received 16 July 2003; received in revised form 5 August 2003

Abstract

The phenomenon of stochastic resonance has recently been found in many systems. Despite the pre-conception of a destructive role of noise, its constructive role has been recognised, in particular in amplification of weak external signals, thereby facilitating signal detection and transduction in complex systems. Although the stochastic resonance has been reported for many systems in various fields of physics, chemistry and biology, the understanding of this phenomenon is still limited. In the present paper, we explain the frequency dependent stochastic resonance with the local divergence. In a model for intracellular Ca^{2+} oscillations, we calculate the local divergence of noise-induced oscillations and show that areas of attractors with close to zero local divergence are crucial for understanding the stochastic resonance, since they represent the most flexible and susceptible states of the system, which are thus most likely to be altered by weak external stimuli and noise. With a detailed analysis of the temporal evolution of the local divergence, we are able to explain the constructive as well as the destructive role of noise, thereby shedding light on the typical bell-shaped dependency of the signal-to-noise ratio vs. the noise intensity. The applicability of our results to other systems and their biological implications are discussed.

© 2003 Elsevier B.V. All rights reserved.

PACS: 87.16.Ac; 87.16.Xa; 05.40.–a

Keywords: Stochastic resonance; Local divergence; Calcium oscillations

* Corresponding author. Tel.: +386-2-2293643; fax: +386-2-2518180.
E-mail address: marko.marhl@uni-mb.si (M. Marhl).

1. Introduction

Stochastic processes are a part of real life. Usually, noisy fluctuations are considered as destructive, hard eliminable components of complex processes. For example, in electronic circuits noise is known to impair signal detection and transduction. However, in the past 10 years many experimental evidences were provided revealing a constructive role of noise. Already in 1993, Douglass et al. [1] found that in the mechanoreceptors of crayfish tails, noisy environment caused by thermal fluctuations improves the detection of water currents evoked by a predator. Similar results were obtained by Braun et al. [2] who found that noisy background improves the sensitivity of shark sensory cells. Moreover, noise was successfully used in a clinical application for helping humans with impaired hearing. Morse and Evans [3] suggested that noise could be artificially added to a cochlear implant to improve its functionality. Recently, Manjarrez et al. [4] reported about the noise-induced coherence between spinal and cortical neuronal ensembles in a cat. For human brain, it has been shown that the electroencephalographic responses evoked by mechanical tactile stimuli can be optimised by adding noise [5].

In order to explain the constructive role of noise, many theoretical studies have been devoted to examine the effects of noise and other weak external stimuli on the behaviour of dynamical systems. It has been shown that noise enhances, i.e., amplifies, weak input signals and herewith facilitates detection and transduction of weak signals. The constructive role of noise depends in a resonance-like manner on the noise intensity. This phenomenon, known as stochastic resonance, has been reported in a broad variety of physical [6], chemical [7,8], and biological systems [9–15]. For a comprehensive review see Ref. [16]. The stochastic resonance is predominantly encountered in bistable systems, where the transitions between two coexisting states are induced by noise. However, stochastic resonance was also reported in the vicinity of Hopf bifurcations [17–20], where the constructive role of stochastic influences is related to the noise stimulated transitions between two quasi-stationary dynamical states.

In some cases stochastic resonance phenomena can be observed in the absence of any deterministic external inputs, thus they are induced solely by noise [21–26]. It has been shown that without external deterministic inputs coherence of noise-induced oscillations is maximized for an optimal level of noise intensity. This phenomenon was termed as coherence resonance [23–25], or internal stochastic resonance [26]. Furthermore, the phenomenon of coherence resonance was also reported in the absence of external stochastic inputs, thus induced solely by the presence of internal noise [27–29]. This phenomenon, termed as intrinsic coherence resonance [27], originates from stochastic opening and closing of individual ion channels due to thermal fluctuations, thus introducing intrinsic noise into the membrane potential of the cell, whereas the noise intensity at which the most regular cell activity can be found is determined by the size of ion channel clusters [28]. In particular, clustering of calcium release channels into appropriate sizes increases the sensitivity of calcium responses, thereby optimising intracellular calcium signalling in many cell types [29].

The existence of internal stochastic resonance in a dynamical system predominantly indicates that the system has a preferred oscillation frequency, i.e., characteristic time scale, which is present in the system for all noise intensities. This preferred

oscillation frequency characterises the dynamics of the system even in the presence of continuous external stimuli. Thus, the ability of the system to respond synchronously to a periodic external signal is rather small, and the characteristic time scale remains largely present in the system despite external influences (see Ref. [30]). Therefore, such systems mostly possess very low frequency variability, which is often in contradiction with experimentally observed features of many biological systems, like for example behaviour of neuron ensembles [31] or gene expression and enzymatic activities [32,33].

Although noise undoubtedly has a constructive role in various dynamical systems, only few studies were aimed to explaining these phenomena [15,30]. It is widely agreed that noise amplifies deterministic input signals, so that the probability of crossing a threshold of a bifurcation point increases. Thereby, noise-induced oscillations come into existence, which at certain noise intensity have the best correlation with the deterministic input signal. In case of internal stochastic resonance, the noise itself is considered as a suprathreshold external signal, which causes the system to oscillate with its characteristic frequency. The constructive roles of noise are mostly measured by calculating the so-called signal-to-noise ratio (SNR) (see Ref. [35]). The SNR measures the level of determinism that is present in the system for various noise intensities. For example, if the system is forced with a continuous subthreshold signal that has a well-defined frequency, the SNR measures how much of this frequency is present in the response of the system at various noise intensities. Typically, the obtained results show a resonance like dependency of the SNR on the noise intensity.

Recently, several studies were devoted to studying the SNR for dynamical systems in the presence of noise and deterministic external stimuli with various forcing frequencies [15,36–39]. It has been shown that some dynamical systems are able to respond coherently to subthreshold external signals with various forcing frequencies if noise with an optimal frequency dependent intensity is added [15,37,39]. This phenomenon was termed as frequency dependent stochastic resonance [15]. The main property of the frequency dependent stochastic resonance is that the noise intensity at which the peak SNR value is obtained depends crucially on the frequency of the input signal. Despite the fact, that the frequency dependent stochastic resonance was reported by several authors, the understanding of this interesting phenomenon is still very limited.

The aim of the present study is to explain the frequency dependent stochastic resonance in a mathematical model for intracellular Ca^{2+} oscillations proposed by Marhl et al. [40]. We investigate the responses of the examined mathematical model to noise and subthreshold periodic input signals in the vicinity of a subcritical Hopf bifurcation. By applying solely suprathreshold noise to the system, the latter doesn't express any preferred oscillation frequency, and is thus characterised by high frequency variability. Therefore, for various noise intensities, the system is able to oscillate coherently with subthreshold periodic input signals in a wide frequency range. In order to achieve the best coherence between the system output and the external periodic signal with different forcing frequencies, different optimal noise intensities are required. This is a characteristic property of the frequency dependent stochastic resonance. To explain this frequency dependent stochastic resonance, we calculate the time course of local divergence for noise-induced oscillations. We focus on parts of attractors with close to

zero local divergence and study the effects of noise and the subthreshold deterministic input signals on these parts. Separately, we study the constructive and the destructive role of noise, and are herewith able to explain the ascending as well as the descending part of the resonance dependency of the SNR vs. the noise intensity. The basic intuitive idea is that parts of attractors with close to zero local divergence are weakly attractive and can therefore be most easily modified by external signals. The modification of the basic attractor with a subthreshold deterministic signal is only possible if in addition to the subthreshold forcing also weak noise is introduced to the system. The added noise reduces the threshold and acts as an amplifier of the weak external signal. This is the constructive role of noise. By increasing the noise intensity beyond the optimal value, noise becomes destructive. This is due to the fact that at higher noise intensities, noise alone becomes a suprathreshold signal and is thus able to modify the basic attractor. Since the system has the lowest threshold in the most flexible parts of the attractor, which are characterised by close to zero local divergence, studying the local divergence is of much importance in explaining the stochastic resonance effects.

The paper is structured as follows. Section 2 is devoted to the formal description of the examined mathematical model. In Section 3 we present the obtained results. Finally, in the last section we discuss possible biological implications of the results and briefly compare them with results obtained in other systems with different properties than studied in this paper.

2. Mathematical model

We use a mathematical model for intracellular Ca^{2+} oscillations, originally proposed by Marhl et al. [40]. The model consists of three basic model compartments, i.e., the cytosol, the endoplasmic reticulum (ER), and the mitochondria (for details see Ref. [40]). Consequently, the three main variables are: free Ca^{2+} concentration in the cytosol (Ca_{cyt}), free Ca^{2+} concentration in the ER (Ca_{er}), and free Ca^{2+} concentration in the mitochondria (Ca_{m}). The evolution of the model system is governed by the following differential equations:

$$\frac{dCa_{\text{cyt}}}{dt} = J_{\text{ch}} - J_{\text{pump}} + J_{\text{leak}} + J_{\text{out}} - J_{\text{in}} + J_{\text{CaPr}} - J_{\text{Pr}}, \quad (1)$$

$$\frac{dCa_{\text{er}}}{dt} = \frac{\beta_{\text{er}}}{\rho_{\text{er}}} (J_{\text{pump}} - J_{\text{ch}} - J_{\text{leak}}), \quad (2)$$

$$\frac{dCa_{\text{m}}}{dt} = \frac{\beta_{\text{m}}}{\rho_{\text{m}}} (J_{\text{in}} - J_{\text{out}}), \quad (3)$$

where

$$J_{\text{ch}} = k_{\text{ch}} \frac{Ca_{\text{cyt}}^2}{Ca_{\text{cyt}}^2 + K_1^2} (Ca_{\text{er}} - Ca_{\text{cyt}}), \quad (4)$$

$$J_{\text{pump}} = k_{\text{pump}} Ca_{\text{cyt}} , \quad (5)$$

$$J_{\text{leak}} = k_{\text{leak}} (Ca_{\text{er}} - Ca_{\text{cyt}}) , \quad (6)$$

$$J_{\text{Pr}} = k_{+} Ca_{\text{cyt}} Pr , \quad (7)$$

$$J_{\text{CaPr}} = k_{-} CaPr , \quad (8)$$

$$J_{\text{in}} = k_{\text{in}} \frac{Ca_{\text{cyt}}^8}{Ca_{\text{cyt}}^8 + K_2^8} , \quad (9)$$

$$J_{\text{out}} = \left(k_{\text{out}} \frac{Ca_{\text{cyt}}^2}{Ca_{\text{cyt}}^2 + K_1^2} + k_{\text{m}} \right) Ca_{\text{m}} . \quad (10)$$

Concentrations of the free (Pr) and the occupied ($CaPr$) protein binding sites are given by two conservation relations (see Ref. [40]):

$$Pr = Pr_{\text{tot}} - CaPr , \quad (11)$$

$$CaPr = Ca_{\text{tot}} - Ca_{\text{cyt}} - \frac{\rho_{\text{er}}}{\beta_{\text{er}}} Ca_{\text{er}} - \frac{\rho_{\text{m}}}{\beta_{\text{m}}} Ca_{\text{m}} . \quad (12)$$

To study the effects of noise and subthreshold external periodic inputs on the behaviour of the model system, we use the additive Gaussian noise ($\zeta(t)$) with the standard deviation σ and zero mean value, and the periodic pulse train ($f(t)$) defined as

$$f(t) = \begin{cases} a & \text{if } (t \bmod v_f^{-1}) > (v_f^{-1} - d) , \\ -a & \text{if } ((t - d) \bmod v_f^{-1}) > (v_f^{-1} - d) , \\ 0 & \text{else ,} \end{cases} \quad (13)$$

where v_f is the oscillation frequency, d is the duration and a is the amplitude of the periodic pulse trains. Both the additive Gaussian noise ($\zeta(t)$) and the periodic pulse train ($f(t)$) are introduced to the model system as additional Ca^{2+} fluxes through the cell membrane. Thus Eq. (1) obtains two additional terms in form of $\zeta(t)$ and $f(t)$. Due to these additional Ca^{2+} fluxes, the total concentration of calcium in the cell (Ca_{tot}) is no longer constant. An additional differential equation is needed for calculating changes in the total Ca^{2+} concentration in the cell:

$$\frac{dCa_{\text{tot}}}{dt} = f(t) + \zeta(t) . \quad (14)$$

The complete set of model equations is given by Eqs. (1)–(14). In the paper, all results are calculated for the parameter values given in caption of Fig. 1 if not otherwise stated, whereas a complete presentation of their meaning and biological relevance is given in Ref. [40].

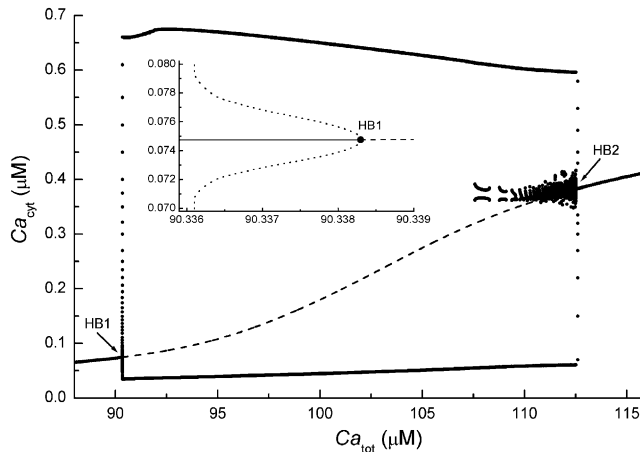


Fig. 1. Bifurcation diagram of the examined mathematical model without inclusion of noise and external deterministic stimuli. Parameter values are: $k_{ch}=469 \text{ s}^{-1}$, $k_{leak}=0.05 \text{ s}^{-1}$, $k_{pump}=20 \text{ s}^{-1}$, $k_{in}=300 \mu\text{M s}^{-1}$, $k_{out}=125 \text{ s}^{-1}$, $k_m=0.00625 \text{ s}^{-1}$, $k_+=0.1 \mu\text{M}^{-1} \text{ s}^{-1}$, $k_-=0.01 \text{ s}^{-1}$, $K_1=5.0 \mu\text{M}$, $K_2=0.8 \mu\text{M}$, $P_{r_{tot}}=120 \mu\text{M}$, $\rho_{er}=0.01$, $\beta_{er}=0.0025$, $\rho_m=0.01$, $\beta_m=0.0025$.

3. Results

To determine basic dynamical properties of the model system (Eqs. (1)–(12)) without applying $\zeta(t)$ and $f(t)$, we carry out the bifurcation analysis. Since $\zeta(t)$ and $f(t)$ affect the total concentration of calcium in the cell, it is reasonable to choose Ca_{tot} as the bifurcation parameter. The bifurcation diagram of Ca_{cyt} vs. Ca_{tot} is presented in Fig. 1. For different values of Ca_{tot} the examined mathematical model exhibits various types of Ca^{2+} oscillations from simple spiking to chaotic bursting oscillations. The oscillatory regime starts and ends with a subcritical Hopf bifurcation (HB1 and HB2 in Fig. 1) at $Ca_{tot}=90.3384 \mu\text{M}$ and $Ca_{tot}=112.552 \mu\text{M}$, respectively. We focus on the vicinity of HB1. Therefore, we set the initial value for Ca_{tot} in Eq. (14) at $90.0 \mu\text{M}$. Note that for this value of Ca_{tot} only a stable steady state exists (see inset of Fig. 1). Thus, if no $\zeta(t)$ or $f(t)$ is applied to the system, the system cannot oscillate for any initial conditions.

We start by examining solely the effects of noise on the behaviour of the model system, i.e., we apply noise of various intensities (σ). In Fig. 2, time courses of Ca_{cyt} for various σ are presented. For small noise intensities, the threshold for the oscillatory regime is not reached and the system remains quiescent. For higher values of σ , first only few spikes emerge, whereas for even higher noise intensities a predominant oscillation frequency of the noise-induced oscillations rises significantly (see Fig. 2).

Results in Fig. 2 show that the system has no characteristic time scale or preferred oscillation frequency if solely noise is introduced to the system. In fact, by changing the noise intensity almost any oscillation frequency of the system may be obtained. This assures high frequency variability of the system in a wide frequency range. To confirm

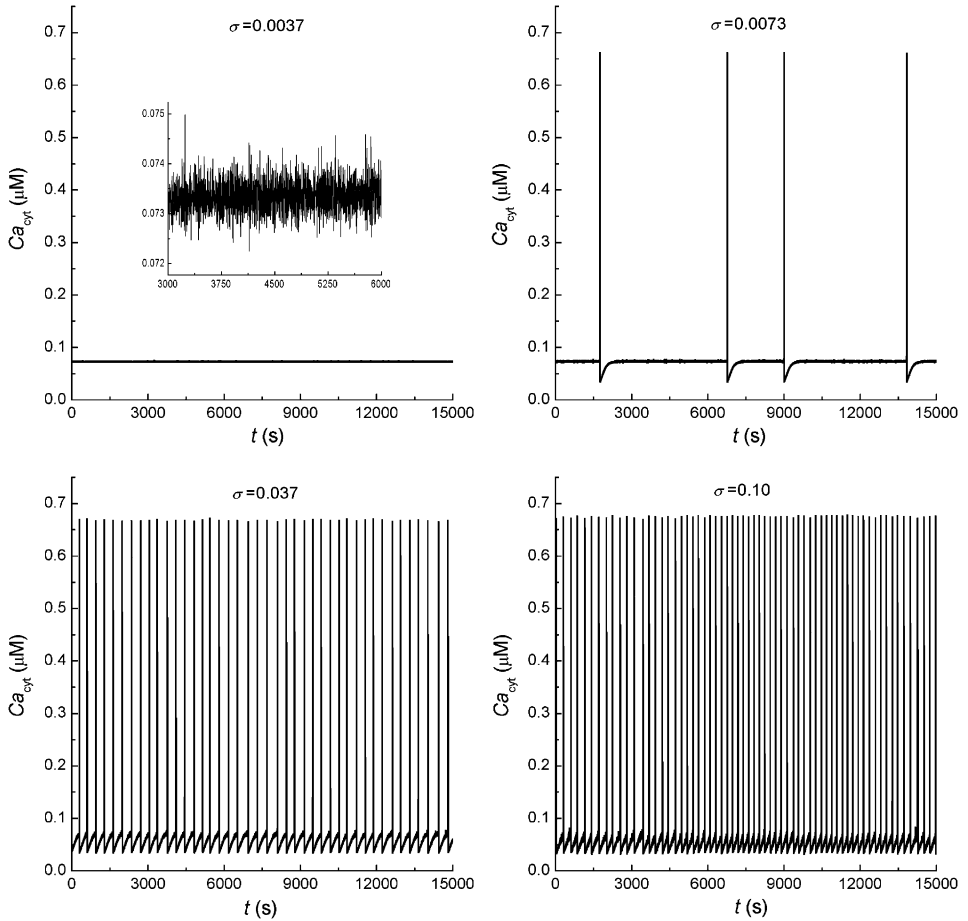


Fig. 2. Solely noise induced oscillations for several values of σ .

this mathematically, we calculate the power spectra of noise-induced oscillations for different values of σ . The results presented in Fig. 3 show that an almost continuous frequency distribution can be obtained by varying σ . This confirms that the examined mathematical model is indeed characterized by extremely high frequency variability.

Since the system possesses high frequency variability, it remains of interest to investigate if this property assures the system to respond flexibly to weak external periodic stimuli, i.e., if the system is able to adjust its frequency in response to an external signal. To this purpose, in addition to the Gaussian noise, we introduce the small-amplitude external periodic forcing $f(t)$ (see Eq. (13)), and examine the system ability to oscillate synchronously, i.e., with the same frequency as the external signal. For all calculations, we choose $a = 0.001 \mu\text{M s}^{-1}$ and $d = 0.012\nu_f^{-1}$, whereas the external signal frequency (ν_f) is given in figure captions. Note that the chosen initial

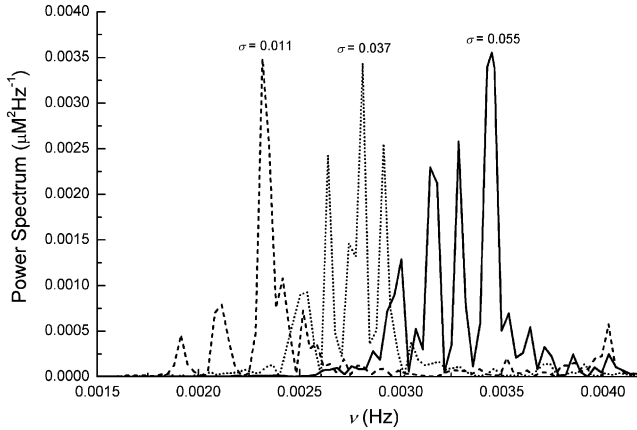


Fig. 3. Power spectrums of solely noise induced oscillations for several values of σ .

value $Ca_{\text{tot}} = 90.0 \mu\text{M}$ and the value of Ca_{tot} at the bifurcation point HB1 of the basic model system are so much apart (see inset of Fig. 1) that the periodic pulse train $f(t)$ alone cannot induce any oscillations, and is thus considered as a subthreshold signal. Therefore, only if $\sigma > 0$, noise-induced oscillations can appear. In Fig. 4, we show time courses of Ca_{cyt} together with $f(t)$ for various σ . It can be seen that an optimal noise intensity exist for which the system is almost 1:1 synchronised with the external signal. Fig. 4 shows that for small σ only few spikes emerge. It should be noted, however, that each spike exactly matches one of the spikes of the periodic pulse trains. This gives the output signal a deterministic character. On the other hand, for larger σ the effect of noise becomes predominant and the system begins oscillating in a stochastic manner, independently of the frequency of the periodic pulse trains.

To quantify mathematically the deterministic/stochastic nature of the system's response to $\zeta(t)$ and $f(t)$, we calculate the autocorrelation function for the three time series of Ca_{cyt} presented in Fig. 4. The autocorrelation function ($\chi(\tau)$) can be calculated according to the definition:

$$\chi(\tau) = \lim_{t \rightarrow \infty} \frac{1}{t} \int_0^t Ca_{\text{cyt}}(t + \tau) Ca_{\text{cyt}}(t) dt . \quad (15)$$

In addition to the autocorrelation function also the normalised interspike interval histograms (ISIH) were calculated. Both, the autocorrelation function and the ISIH are commonly used methods (see for example Ref. [15]) for quantifying the deterministic nature as well as for determining the predominant oscillation frequency of a time series.

The autocorrelation functions and the ISIH for the Ca_{cyt} time series in Fig. 4 are presented in Fig. 5. For lower σ , the deterministic nature of the Ca_{cyt} time series is clearly legible. However, due to the low noise intensity, the system rarely responds to the deterministic subthreshold periodic signal, and the autocorrelation of the signal is therefore rather weak. This is confirmed by the ISIH which shows almost equally

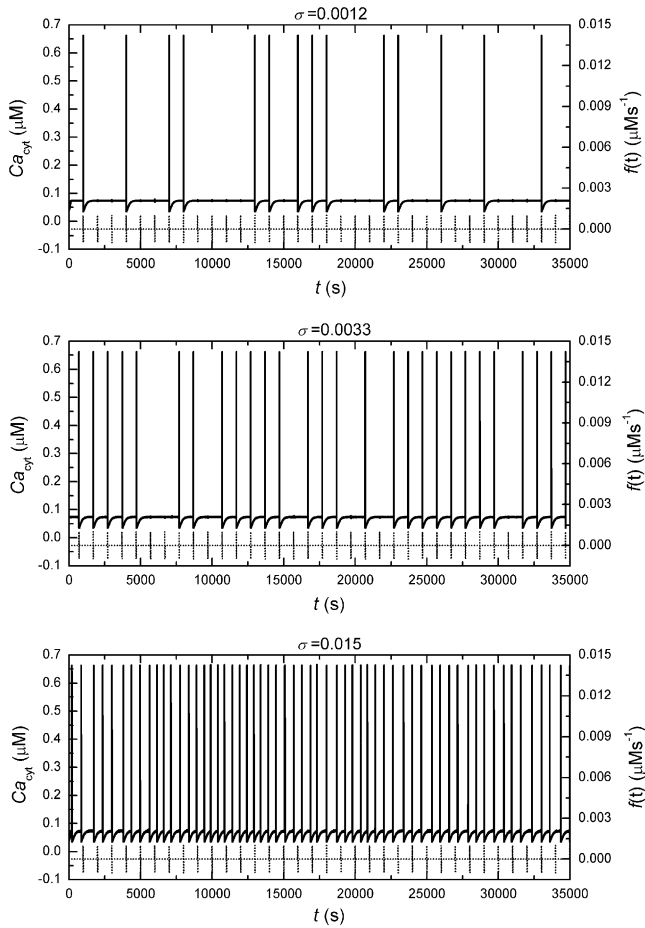


Fig. 4. Temporal evolution of Ca_{cyt} for several values of σ when an external periodic pulse train with $a = 0.001$ and $\nu_f = 1.00e^{-3}$ Hz is applied.

distributed maximums at integer multiples of the forcing period. For the optimal noise intensity (middle part of Fig. 5), the deterministic input is amplified enough to provoke Ca_{cyt} spikes at almost all spikes of the input signal $f(t)$. Consequently, the corresponding autocorrelation is very high, and the ISIH has a very concentrated maximum at the forcing frequency, with some lower peaks at its higher harmonics. By increasing σ over the optimal value, the periodic input is amplified even further, however, the deterministic influence of the periodic pulse trains is completely blurred by noise (see lower part of Fig. 5). This shows that the optimal response of the system results from a kind of competition between the noise and the periodic input. If σ is too small, the deterministic input signal is not amplified enough and the system doesn't respond to every spike of the pulse train; if the noise intensity is too high, the external

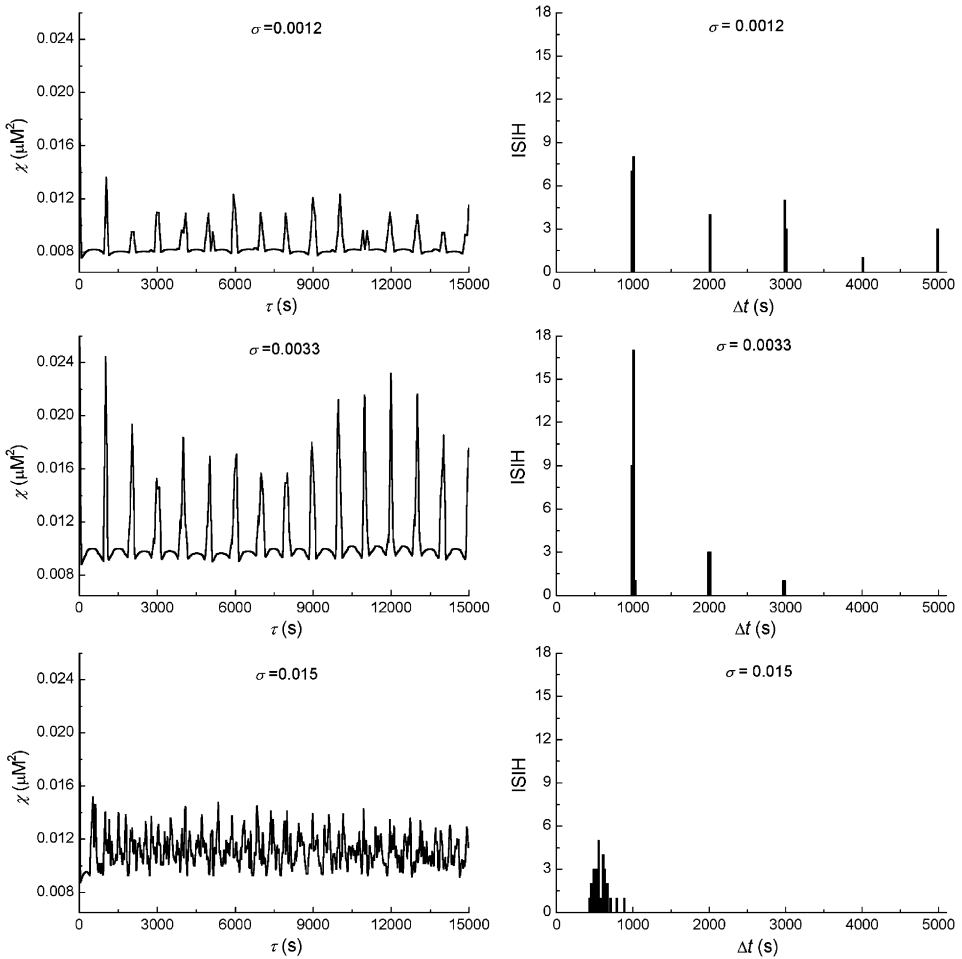


Fig. 5. Autocorrelation function and the normalised interspike interval histograms (ISIH) for the Ca_{cyt} time courses presented in Fig. 4.

periodic signal is completely overruled by noise and the synchronisation with the external periodic signal is completely lost.

Results in Figs. 4 and 5 show that noise plays a crucial role in amplifying the deterministic subthreshold input signal and has a constructive role in assuring the coherence between the system's output and the input signal. To quantify the constructive role of noise, we calculate the SNR. For calculating the SNR, we take use of a definition originally proposed by Palm et al. [41]. They defined a correlation coefficient (C) between the pulse train and the output time series of the system. Both time series are divided into n bins with width δ , whereas the number of pulses in the i -th bin is denoted by X_i and Y_i for the pulse train and the time series of Ca_{cyt} , respectively. The width δ

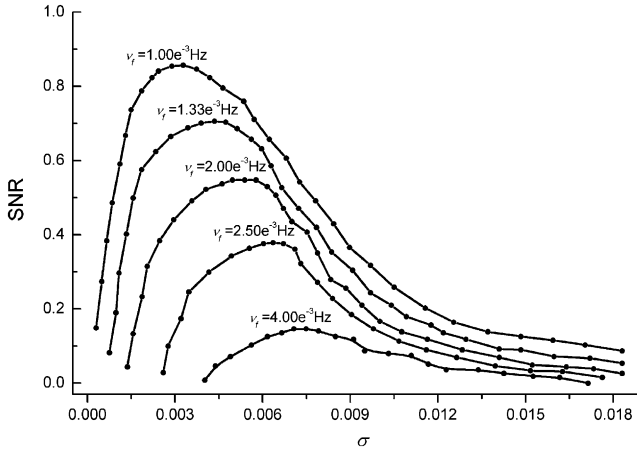


Fig. 6. The SNR in dependence on σ for various frequencies of the external periodic pulse trains.

is set small enough so that X_i and Y_i can only take the value 0 or 1. The correlation coefficient C is defined as [41]

$$C = \frac{Z - (\sum_i X_i Y_i)/n}{\sqrt{\sum_i X_i (1 - (\sum_i X_i/n)) \sum_i Y_i (1 - (\sum_i Y_i/n))}}, \tag{16}$$

where Z is the number of coincident firings. In our case, the calculations were made for very long time series so that $n \rightarrow \infty$. Applying this to Eq. (16), we obtain the following equation for calculating the SNR:

$$\text{SNR} = \frac{Z}{\sqrt{\sum_i X_i \sum_i Y_i}}, \tag{17}$$

where all symbols have the same meaning as in Eq. (16). Similar measures for quantifying the SNR were already used previously by Kanamaru and Okabe [12], and Reinker et al. [15], for example.

Using Eq. (16), we calculate the SNR for various oscillation frequencies of the pulse train (ν_f). In Fig. 6, the results are presented for $\nu_f = 1.00e^{-3}$ Hz, $\nu_f = 1.33e^{-3}$ Hz, $\nu_f = 2.00e^{-3}$ Hz, $\nu_f = 2.50e^{-3}$ Hz, and $\nu_f = 4.00e^{-3}$ Hz. It can be seen that the resonance peak for lower pulse train frequencies occurs at lower noise intensity, whereas for higher frequencies of the pulse train the resonance peak occurs at higher noise intensity. This is a typical example of frequency dependent stochastic resonance, which was previously encountered only in neural systems (see Refs. [15,36–39]). Another important feature of the results presented in Fig. 6 is a significant decrease in the height of the SNR peaks, which sets in for higher pulse train frequencies (ν_f).

Taken together, in Fig. 6 we showed that the height of the SNR peak value as well as the noise intensity at which this peak occurs depend crucially on the oscillation frequency of the periodic pulse trains. Moreover, we showed that Ca_{cvt} oscillations, presented in Fig. 4, have a deterministic nature for lower noise intensities, which is best expressed at the SNR peak value (see middle part of Fig. 5), whereas at higher

noise intensities this determinism is lost, thus stochastic influences dominate in the behaviour of the system (see lower part of Fig. 5).

To explain these results, we calculate time courses of the local divergence for the noise-induced oscillations. In our previous works [42,43], we showed that the divergence could be taken as a measure for estimating the system's ability to respond synchronously to an external signal. We showed that close to zero divergence largely facilitates the flexibility of the system, thus enabling it to respond coherently to weak external signals. Since in the present study, Gaussian noise and the periodic pulse train are considered as external signals, the same reasoning could also be used for explaining the above-presented results. We calculate the local divergence for the vector field:

$$\begin{aligned} \mathbf{F}(Ca_{\text{cyt}}, Ca_{\text{er}}, Ca_{\text{m}}, Ca_{\text{tot}}) &= (F_{Ca_{\text{cyt}}}, F_{Ca_{\text{er}}}, F_{Ca_{\text{m}}}, F_{Ca_{\text{tot}}}) \\ &= \left(\frac{dCa_{\text{cyt}}}{dt}, \frac{dCa_{\text{er}}}{dt}, \frac{dCa_{\text{m}}}{dt}, \frac{dCa_{\text{tot}}}{dt} \right) \end{aligned} \quad (18)$$

according to the definition:

$$\nabla \cdot \mathbf{F}(Ca_{\text{cyt}}, Ca_{\text{er}}, Ca_{\text{m}}, Ca_{\text{tot}}) = \frac{\partial F_{Ca_{\text{cyt}}}}{\partial Ca_{\text{cyt}}} + \frac{\partial F_{Ca_{\text{er}}}}{\partial Ca_{\text{er}}} + \frac{\partial F_{Ca_{\text{m}}}}{\partial Ca_{\text{m}}} + \frac{\partial F_{Ca_{\text{tot}}}}{\partial Ca_{\text{tot}}}, \quad (19)$$

where $(Ca_{\text{cyt}}, Ca_{\text{er}}, Ca_{\text{m}}, Ca_{\text{tot}})$ is a point on the attractor.

First, we calculate the local divergence for the solely noise induced oscillations presented in Fig. 2. The upper part of Fig. 7 shows the time course of the local divergence for oscillations induced by weak noise ($\sigma=0.0073$). Large areas with close to zero local divergence are well expressed. In accordance to our previous studies [42,43], the system is highly flexible in such areas and is thus able to respond even to extremely weak external signals. On the other hand, parts with highly negative local divergence represent the most rigid areas that are difficult to modify even with high noise intensities. Since parts with close to zero local divergence are highly susceptible to external signals, noise with increasingly higher intensities ($\sigma=0.037$ and 0.10) is able to provoke more and more new spikes. Thereby, the frequency of the noise-induced Ca^{2+} oscillations rises at higher σ , as shown in Fig. 2. In fact, noise with higher σ cuts the flexible parts of the time course, and consequently the susceptible parts with close to zero local divergence areas disappear (see Fig. 7).

Moreover, calculations of the local divergence enable us to explain the phenomenon of the stochastic resonance presented in Fig. 6. Curves in Fig. 6 have a typical bell-shaped form, showing that weak noise has a constructive role, whereas higher noise intensities destruct coherent system responses. Fig. 8 shows the local divergence of the time courses presented in Fig. 4, i.e., time courses before the resonance peak, at the peak and after the peak. At lower σ , noise acts as an amplifier of the deterministic input signals, which results in the appearance of first spikes, as shown in the upper part of Fig. 4. For this case, the time course of the local divergence is characterised by extensive regions of close to zero local divergence (see Fig. 8), which in accordance with our previous statements expresses high flexibility of the system. By further enhancing the noise intensity, the excitability of the system rises, and thus the probability of evoking new Ca_{cyt} spikes by the periodic pulse train becomes higher. Eventually,

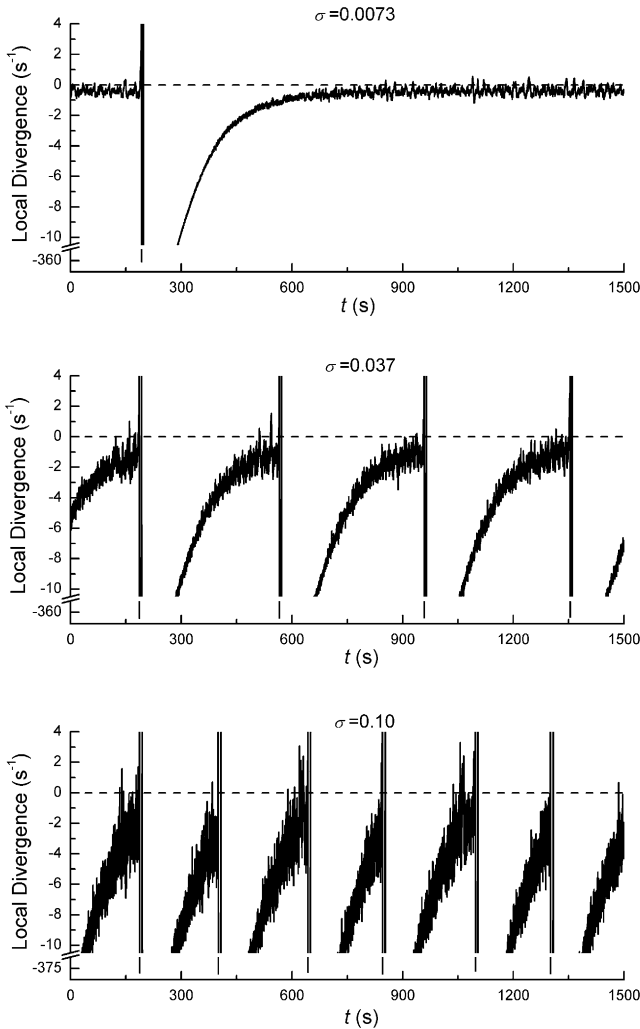


Fig. 7. Temporal evolution of the local divergence for solely noise induced oscillations at several values of σ .

this leads to the resonant response of the system in which the best compromise between the noise intensity and the external periodic signal is found. At the peak SNR value, noise enhances the excitability of regions with close to zero local divergence to a degree at which noise itself cannot evoke spikes, however, enables the weak external periodic signal to evoke Ca_{cyt} spikes at almost all peaks of the $f(t)$ (see middle part of Fig. 8). Under such conditions, the excitability of flexible regions with close to zero local divergence is optimally tuned with respect to the forcing signal. If namely the noise is further enhanced, the noise itself can force the system to fire spikes, which

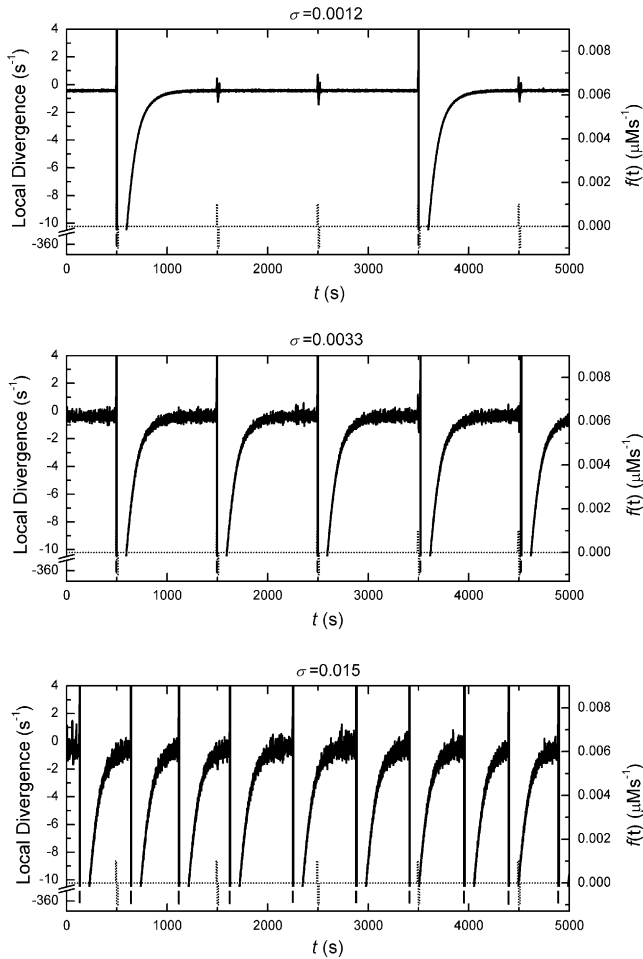


Fig. 8. Temporal evolution of the local divergence for several values of σ when an external periodic pulse train with $a = 0.001$ and $\nu_f = 1.00e^{-3}$ Hz is applied.

reduces the coherency between the system's response and the external periodic signal (see lower part of Fig. 8).

Furthermore, the calculations of the local divergence (Figs. 7 and 8) enable us to explain lowering and shifting of the peak SNR values in Fig. 6 to higher σ if higher frequencies of the external periodic signal are applied. Since the local divergence is not constantly close to zero at the highly susceptible parts of the time course but slightly approaches the zero value (see Fig. 7), increasingly larger noise intensities are required to make the system optimally excitable for higher frequencies of the periodic pulse trains. Therefore, in Fig. 6, the peak SNR values are shifted to higher σ for higher pulse train frequencies. Concomitantly, the higher noise intensities required for

the optimal level of excitability for higher frequencies of the periodic pulse trains reduce the coherent responses of the system. This is because the border between the random effects of noise and the deterministic influences of the periodic pulse trains with the given constant amplitude becomes increasingly effaced as the noise intensity rises, and thus the maximum value of the SNR decreases by increasing forcing frequencies. Therefore, the peak SNR values become smaller at higher forcing frequencies as shown in Fig. 6.

4. Discussion

In this paper, we investigated the responses of a mathematical model for intracellular Ca^{2+} oscillations to deterministic external stimuli with various oscillation frequencies in the presence of Gaussian noise. We have shown that the system doesn't possess a characteristic time scale, i.e., a preferred oscillation frequency. In fact, with various noise intensities a broad and almost continuous frequency spectrum can be obtained. This high frequency variability enables the system to adjust its oscillation frequency to various subthreshold external stimuli. Since different frequencies of the external stimuli require different noise intensities for best correlation (highest SNR) between the pulse train and the output of the system, the examined mathematical model exhibits a typical frequency dependent stochastic resonance.

In order to explain the obtained results we have calculated the time course of local divergence for the noise-induced oscillations. The interrelation between local divergence and the susceptibility of the system to external influences seems reasonable, since the local divergence represents the spatial attractive properties of the system's attractor. Therefore, in areas where the local divergence is close to zero, the system is very susceptible and is able to respond even to very weak external signals. On the other hand, highly negative local divergence areas characterise very rigid non-flexible states of the system, which can be only little altered by external signals. We used the same reasoning in our previous articles [42,43] to explain the system ability to respond synchronously to an external periodic forcing signal.

The presented results in Figs. 7 and 8 show that in order to achieve good correlations between the system's output and the high frequency deterministic external stimuli, the system has to be altered in increasingly low local divergence areas. Consequently, higher noise intensities are required to amplify the subthreshold periodic signal strong enough to provoke such high-frequency spikes of the system. Hence, the peak values of the SNR in Fig. 6 are shifted to higher noise intensities as the frequency of the periodic pulse trains increases. Furthermore, due to the higher noise intensities required for such high-frequency correlations, also the maximum value of the SNR decreases, since the deterministic step-like shape of the periodic pulse trains is increasingly overruled, i.e., blurred by noise. Therefore, the majority of evoked spikes are provoked randomly, and the response of the system is thus much weaker correlated with the periodic pulse train.

Frequency dependent stochastic resonance was previously reported for the Hindmarsh–Rose neuron model by Reinker et al. [15]. In order to explain their results, they calculated the complex impedance of the model and obtained one single

singularity, i.e., impedance maximum, at a certain system frequency. However, the highest peak SNR value achieved at the lowest noise intensity was obtained at a significantly lower external forcing frequency as suggested by their mathematical analysis. Nevertheless, they provided an intuitive explanation for their results, suggesting that the high frequency external forcing requires higher noise intensity in order to have the same likelihood of crossing the system's threshold in a shorter amount of time. Our preliminary calculations of the local divergence for the Hindmarsh–Rose neuron model show that the same reasoning as applied for explaining the results in the present paper can also be used to explain the frequency dependent stochastic resonance in Ref. [15].

Furthermore, by calculating the local divergence for the Fitzhugh–Nagumo neuron model we can explain the robustness of the system reported previously by Massané and Vicente [30]. They showed that the Fitzhugh–Nagumo neuron model possesses an internal characteristic time scale, which remains largely present in the system for all external forcing frequencies. Our preliminary studies show that the system investigated in Ref. [30] is characterized by extensive highly negative local divergence areas with almost no regions with close to zero divergence for system's states in the vicinity of the supercritical Hopf bifurcation that marks the transition between the stationary and the oscillatory regime. Therefore, if the applied forcing frequency is significantly different from the internal characteristic oscillation frequency of the system, it is virtually impossible to amplify the subthreshold periodic signal high enough so that the forcing frequency would be the predominant one in the system. Only if very high noise intensities are applied, the deterministic forcing signal is able to provoke oscillations, which are, however, due to the required higher noise intensity completely uncorrelated with the forcing signal, and thus express a stochastic nature, with the system's internal frequency background, which manifests clearly in the calculated power spectra in Ref. [30].

Authors in Ref. [30] also report, that a high degree of internal coherence is biological undesirable, since it predicts high robustness, preventing the system to respond efficiently to external changes, thereby perceiving only little information from the environment. Moreover, results in Ref. [30] show that in such cases, even at the peak SNR value, the frequency distribution of the system's response is much more broad and diffuse; even more so if the forcing frequency is largely different from the characteristic internal frequency of the system. From the biological point of view, such signal transduction is inefficient, since it carries less biologically relevant information. On the other hand, the model studied in this paper expresses high frequency variability, which enables it to respond synchronously to various forcing frequencies (see Fig. 6). Furthermore, the frequency distribution of the system's output at the peak SNR value is extremely concentrated around the forcing frequency (see Fig. 5). This is of special biological importance, since biologically relevant information is known to be predominantly frequency encoded (see Refs. [32–34,44–47]). Since in general, the characteristic internal time scale is found predominantly in the vicinity of supercritical Hopf bifurcations [26,30], it remains of interest to investigate the potential biological relevance of different bifurcation types that can be encountered in biological systems [48,49]. Our results indicate that subcritical Hopf bifurcations with typical hard excitation properties [50] are biologically more relevant, since in the vicinity of such bifurcations oscillations

are characterized with high frequency variability, often combined with low local divergence, which enables the system to respond flexibly to various sub and suprathreshold external signals.

References

- [1] J.K. Douglass, L.A. Wilkens, E. Pantazelou, F. Moss, *Nature* 365 (1993) 337–340.
- [2] H.A. Braun, H. Wissing, K. Schäfer, M.C. Hirsch, *Nature* 367 (1994) 270–273.
- [3] R.P. Morse, E.F. Evans, *Nat. Med.* 2 (1996) 928–932.
- [4] E. Manjarrez, J.G.R. Piloni, I. Mendez, L. Martnez, D. Velez, D. Vazquez, A. Flores, *Neurosci. Lett.* 326 (2002) 93–96.
- [5] E. Manjarrez, O.D. Martnez, I. Mendez, A. Flores, *Neurosci. Lett.* 324 (2002) 213–216.
- [6] L. Gammaitoni, *Phys. Rev. E* 52 (1995) 4691–4698.
- [7] A. Guderian, G. Dechert, K.P. Zeyer, F.W. Schneider, *J. Phys. Chem.* 100 (1996) 4437–4442.
- [8] J. Ross, M.O. Vlad, *Ann. Rev. Phys. Chem.* 50 (1999) 51–78.
- [9] F.C. Blondeau, X. Godivier, N. Chambet, *Phys. Rev. E* 53 (1996) 1273–1275.
- [10] V.V. Osipov, E.V. Ponizovskaya, *Phys. Lett. A* 271 (2000) 191–197.
- [11] T. Kanamaru, Y. Okabe, *BioSystems* 58 (2000) 101–107.
- [12] J. Zhang, F. Qi, H. Xin, *Biophys. Chem.* 94 (2001) 201–207.
- [13] S. Tanabe, K. Pakdaman, *Phys. Rev. E* 64 (2001) 031911.
- [14] P. Hänggi, *Chem. Phys. Chem.* 3 (2002) 285–290.
- [15] S. Reinker, E. Puil, R.M. Miura, *Bull. Math. Biol.* 65 (2003) 641–663.
- [16] L. Gammaitoni, P. Hänggi, P. Jung, F. Marchesoni, *Rev. Mod. Phys.* 70 (1998) 223–287.
- [17] L. Fronzoni, R. Mannella, F. Moss, P.V.E. McClintock, *Phys. Rev. A* 36 (1987) 834–841.
- [18] P. Xing, K. Bachmann, F. Moss, *Phys. Lett. A* 206 (1995) 61–65.
- [19] V.V. Osipov, E.V. Ponizovskaya, *JETP Lett.* 70 (1999) 425–430.
- [20] V.V. Osipov, E.V. Ponizovskaya, *Phys. Rev. E* 61 (2000) 4603–4605.
- [21] H. Gang, T. Ditzinger, C.Z. Ning, H. Haken, *Phys. Rev. Lett.* 71 (1993) 807–810.
- [22] A. Longtin, *Phys. Rev. E* 55 (1997) 868–876.
- [23] A.S. Pikovsky, J. Kurths, *Phys. Rev. Lett.* 78 (1997) 775–778.
- [24] S.G. Lee, A. Neiman, S. Kim, *Phys. Rev. E* 57 (1997) 3292–3297.
- [25] D.E. Postnov, S.K. Han, T.G. Yim, O.V. Sosnovtseva, *Phys. Rev. E* 59 (1999) R3791–R3794.
- [26] S. Zhong, F. Qi, H. Xin, *Chem. Phys. Lett.* 342 (2001) 583–586.
- [27] G. Schmid, I. Goychuk, P. Hänggi, *Europhys. Lett.* 56 (2001) 22–28.
- [28] P. Jung, J.W. Shuai, *Europhys. Lett.* 56 (2001) 29–35.
- [29] J.W. Shuai, P. Jung, *Phys. Rev. Lett.* 88 (2002) 068102.
- [30] S. Massanés, C. Vicente, *Phys. Rev. E* 59 (1999) 4490–4497.
- [31] W.R. Softky, C. Koch, *J. Neurosci.* 13 (1993) 334–350.
- [32] R.E. Dolmetsch, K. Xu, R.S. Lewis, *Nature* 392 (1998) 933–936.
- [33] W.H. Li, J. Llopis, M. Whitney, G. Zlokarnik, R.Y. Tsien, *Nature* 392 (1998) 936–941.
- [34] P. De Koninck, H. Schulman, *Science* 279 (1998) 227–230.
- [35] F. Moss, D. Pierson, D. O’Gorman, *Internat. J. Bifur. Chaos Appl. Sci. Eng.* 4 (1994) 1383–1397.
- [36] T. Shimokawa, K. Pakdaman, S. Sato, *Phys. Rev. E* 59 (1999) 3427–3443.
- [37] B. Lindner, L. Schimansky-Geier, *Phys. Rev. E* 61 (2000) 6103–6110.
- [38] S. Tanabe, K. Pakdaman, *Phys. Rev. E* 64 (2001) 041904.
- [39] J.P. Baltanas, J.M. Casado, *Phys. Rev. E* 65 (2002) 041915.
- [40] M. Marhl, T. Haberichter, M. Brumen, R. Heinrich, *BioSystems* 57 (2000) 75–86.
- [41] G. Palm, A.M.H.J. Aertsen, G.L. Gerstein, *Biol. Cybernet.* 59 (1988) 1–11.
- [42] M. Perc, M. Marhl, *Biophys. Chem.* 104 (2003) 509–523.
- [43] M. Marhl, S. Schuster, *J. Theor. Biol.* 224 (2003) 491–500.
- [44] M. Marhl, S. Schuster, M. Brumen, *Biophys. Chem.* 71 (1998) 125–132.
- [45] V. Grubelnik, A.Z. Larsen, U. Kummer, L.F. Olsen, M. Marhl, *Biophys. Chem.* 94 (2001) 59–74.

- [46] A. Hudmon, H. Schulman, *Biochem. J.* 364 (2002) 593–611.
- [47] K.U. Bayer, P. De Koninck, H. Schulman, *EMBO J.* 21 (2002) 3590–3597.
- [48] E.M. Izhikevich, *Int. J. Bifurcat. Chaos* 10 (2000) 1171–1266.
- [49] M. Perc, M. Marhl, *Chaos, Solitons Fractals* 18 (2003) 759–774.
- [50] S. Schuster, M. Marhl, *J. Biol. Systems* 9 (2001) 291–314.